Individual bioaerosol particle discrimination by multi-photon excited fluorescence

Denis Kiselev,* Luigi Bonacina, Jean-Pierre Wolf

Université de Genève, GAP-Biophotonics,
Rue de l'Ecole de Médecine 20, 1211 Geneva 4, Switzerland
**Denis.Kiselev@unige.ch*

Abstract: Femtosecond laser induced multi-photon excited fluorescence (MPEF) from individual airborne particles is tested for the first time for discriminating bioaerosols. The fluorescence spectra, analysed in 32 channels, exhibit a composite character originating from simultaneous two-photon and three-photon excitation at 790 nm. Simulants of bacteria aggregates (clusters of dyed polystyrene microspheres) and different pollen particles (Ragweed, Pecan, Mulberry) are clearly discriminated by their MPEF spectra. This demonstration experiment opens the way to more sophisticated spectroscopic schemes like pump-probe and coherent control.

OCIS codes: (190.4180) Multiphoton processes; (280.1120) Air pollution monitoring.

References and links

1. Y. L. Pan, J. Hartings, R. G. Pinnick, S. C. Hill, J. Halverson, and R. K. Chang, "Single-particle fluorescence spectrometer for ambient aerosols," Aerosol Sci. Technol. **37**, 628–639 (2003).
2. F. L. Reyes, T. H. Jeys, N. R. Newbury, C. A. Primmerman, G. S. Rowe, and A. Sanchez, "Bio-aerosol fluorescence sensor," Field Anal. Chem. Technol. **3**, 240–248 (1999).
3. J. D. Eversole, W. K. Cary, C. S. Scotto, R. Pierson, M. Spence, and A. J. Campillo, "Continuous bioaerosol monitoring using UV excitation fluorescence: Outdoor test results," Field Anal. Chem. Technol. **5**, 205–212 (2001).
4. G. A. Luoma, P. P. Cherrier, and L. A. Retfalvi, "Real-time warning of biological-agent attacks with the Canadian integrated biochemical agent detection system II (CIBADS II)," Field Anal. Chem. Technol. **3**, 260–273 (1999).
5. Y. L. Pan, K. B. Aptowicz, R. K. Chang, M. Hart, and J. D. Eversole, "Characterizing and monitoring respiratory aerosols by light scattering," Opt. Lett. **28**, 589–591 (2003).
6. P. Kaye, E. Hirst, and Z. WangThomas, "Neural-network-based spatial light-scattering instrument for hazardous airborne fiber detection," Appl. Opt. **36**, 6149–6156 (1997).
7. S. C. Hill, R. G. Pinnick, S. Niles, Y. L. Pan, S. Holler, R. K. Chang, J. Bottiger, B. T. Chen, C. S. Orr, and G. Feather, "Real-time measurement of fluorescence spectra from single airborne biological particles," Field Anal. Chem. Technol. **3**, 221–239 (1999).
8. Y. L. Pan, P. Cobler, S. Rhodes, A. Potter, T. Chou, S. Holler, R. K. Chang, R. G. Pinnick, and J. P. Wolf, "High-speed, high-sensitivity aerosol fluorescence spectrum detection using a 32-anode photomultiplier tube detector," Rev. Sci. Instrum. **72**, 1831–1836 (2001).
9. Y. L. Pan, S. C. Hill, R. G. Pinnick, J. M. House, R. C. Flagan, and R. K. Chang, "Dual-excitation-wavelength fluorescence spectra and elastic scattering for differentiation of single airborne pollen and fungal particles," Atmos. Environ. **45**, 1555–1563 (2011).
10. Y. L. Pan, S. C. Hill, R. G. Pinnick, H. Huang, J. R. Bottiger, and R. K. Chang, "Fluorescence spectra of atmospheric aerosol particles measured using one or two excitation wavelengths: Comparison of classification schemes employing different emission and scattering results," Opt Express **18**, 12436–12457 (2010).
11. V. Sivaprakasam, A. L. Huston, C. Scotto, and J. D. Eversole, "Multiple UV wavelength excitation and fluorescence of bioaerosols," Opt Express **12**, 4457–4466 (2004).
12. J. R. Gord, T. R. Meyer, and S. Roy, "Applications of ultrafast lasers for optical measurements in combusting flows," Annu Rev Anal Chem **1**, 663–687 (2008).

#154559 - $15.00 USD Received 13 Sep 2011; revised 11 Oct 2011; accepted 11 Oct 2011; published 15 Nov 2011

13. J. P. Wolf, F. Courvoisier, V. Boutou, V. Wood, A. Bartelt, M. Roth, and H. Rabitz, "Femtosecond laser pulses distinguish bacteria from background urban aerosols," Appl Phys Lett **87**, 063901 (2005).
14. V. Boutou, F. Courvoisier, L. Guyon, M. Roth, H. Rabitz, and J. P. Wolf, "Discriminating bacteria from other atmospheric particles using femtosecond molecular dynamics," J. Photoch. Photobio. A **180**, 300–306 (2006).
15. H. U. Stauffer, W. D. Kulatilaka, J. R. Gord, and S. Roy, "Laser-induced fluorescence detection of hydroxyl (OH) radical by femtosecond excitation," Opt. Lett. **36**, 1776–1778 (2011).
16. G. Gerber, T. Brixner, N. H. Damrauer, and P. Niklaus, "Photoselective adaptive femtosecond quantum control in the liquid phase," Nature **414**, 57–60 (2001).
17. M. Roth, L. Guyon, J. Roslund, V. Boutou, F. Courvoisier, J. P. Wolf, and H. Rabitz, "Quantum control of tightly competitive product channels," Phys Rev Lett **102**, 253001 (2009).
18. T. Nicolai, D. Carr, S. K. Weiland, H. Duhme, O. von Ehrenstein, C. Wagner, and E. von Mutius, "Urban traffic and pollutant exposure related to respiratory outcomes and atopy in a large sample of children," Eur Respir J **21**, 956–963 (2003).
19. L. Cardenas, S. T. McKenna, J. G. Kunkel, and P. K. Hepler, "NAD(P)H oscillates in pollen tubes and is correlated with tip growth," Plant Physiol. **142**, 1460–1468 (2006).
20. N. Dharajiya, I. Boldogh, V. Cardenas, and S. Sur, "Role of pollen NAD(P)H oxidase in allergic inflammation," Curr. Opin. Allergy Cl **8**, 57–62 (2008).
21. W. W. Webb, W. R. Zipfel, R. M. Williams, R. Christie, A. Y. Nikitin, and B. T. Hyman, "Live tissue intrinsic emission microscopy using multiphoton-excited native fluorescence and second harmonic generation," P. Natl. Acad. Sci. USA **100**, 7075–7080 (2003).
22. S. C. Hill, B. V, J. Yu, S. Ramstein, J. P. Wolf, Y. L. Pan, S. Holler, and R. K. Chang, "Enhanced backward-directed multiphoton-excited fluorescence from dielectric microcavities," Phys. Rev. Lett. **85**, 54–57 (2000).
23. C. Favre, V. Boutou, S. C. Hill, W. Zimmer, M. Krenz, H. Lambrecht, J. Yu, R. K. Chang, L. Woeste, and J. P. Wolf, "White-light nanosource with directional emission," Phys. Rev. Lett. **89**, 035002 (2002).
24. J. Yu, M. Baudelet, L. Guyon, J. P. Wolf, T. Amodeo, E. Frejafon, and P. Laloi, "Femtosecond time-resolved laser-induced breakdown spectroscopy for detection and identification of bacteria: A comparison to the nanosecond regime," J. Appl. Phys. **99**, 084701 (2006).
25. J. Yu, M. Baudelet, M. Bossu, J. Jovelet, J. P. Wolf, T. Amodeo, E. Frejafon, and P. Laloi, "Discrimination of microbiological samples using femtosecond laser-induced breakdown spectroscopy," Appl. Phys. Lett. **89**, 163903 (2006).
26. Y. Silberberg, N. Dudovich, and D. Oron, "Single-pulse coherently controlled nonlinear Raman spectroscopy and microscopy," Nature **418**, 512–514 (2002).
27. A. Dogariu, A. Goltsov, D. Pestov, A. V. Sokolov, and M. O. Scully, "Real-time detection of bacterial spores using coherent anti-stokes Raman spectroscopy," J. Appl. Phys. **103** (2008).
28. S. Roy, P. Wrzesinski, D. Pestov, T. Gunaratne, M. Dantus, and J. R. Gord, "Single-beam coherent anti-Stokes Raman scattering spectroscopy of N_2 using a shaped 7 fs laser pulse," Appl. Phys. Lett. **95** (2009).
29. S. Roy, J. R. Gord, and A. K. Patnaik, "Recent advances in coherent anti-Stokes Raman scattering spectroscopy: Fundamental developments and applications in reacting flows," Prog. Energ. Combust. **36**, 280–306 (2010).

1. Introduction

The detection and identification of bioaerosols, such as airborne bacteria and pollens, have attracted much attention in the last decade. In particular, several optical systems, based on fluorescence [1–4] and/or elastic scattering [5,6] have been developed to distinguish bio- from non-bio aerosols. The most advanced experiments address individual aerosol particles, whose fluorescence is spectrally resolved and analyzed [1, 7, 8]. Dual wavelength excitation (for instance 263 nm and 351 nm) of each particle has emerged [9–11] as an additional tool for improving the measurement selectivity and therefore reducing false alarms. In this letter, we present a novel approach based on multi-photon excited fluorescence (MPEF) of individual bioaerosol particles using femtosecond laser pulses. Thanks to the high peak intensity, 2-photon and 3- photon excited fluorescence (2PEF and 3PEF) from amino acids (tryptophan, tyrosine), NADH, and flavins occur simultaneously, without spectral superposition of excitation and emission. Moreover, the use of femtosecond lasers opens the way to more sophisticated spectroscopic schemes like pump probe experiments [12], which proved efficient for discriminating bioparticles from non-bio particles in solution [13–15] and coherent control, which enabled discriminating between almost identical bio-fluorophors [16, 17].

#154559 - $15.00 USD Received 13 Sep 2011; revised 11 Oct 2011; accepted 11 Oct 2011; published 15 Nov 2011

In the present demonstration experiment, we focused on the MPEF detection of individual pollens (Mulberry, Pecan, Ragweed) and of bacteria simulants (aggregates of 1 μm polystyrene spheres, FluoresBrite PolyFluor 345, Polysciences Inc, referred to an FB345), which exhibit accessible absorption bands for both 2PEF and 3PEF at 790 nm. We used these beads because of their spectral resemblance with the absorption and emission properties of the amino acid tryptophan. The MPEF spectra are resolved in 32 channels in order to gain selectivity, as demonstrated in previous experiments using linear excitation [8]. Increasing interest is currently brought onto pollens due to the hypersensitivity developed by populations in the recent years. This increase of allergic reactions to pollens and asthma may be linked to a simultaneous exposure to airborne pollutants [18]. We decided to compare pollens to simulants of clusters of bacteria (typ. dimensions some tens of micrometers) instead of individual bacteria, since the latter can easily be discriminated by their lower scattering intensity due to their smaller size (typ. 1 μm).

2. Experimental

The experiment (Fig. 1) was inspired by the successful design developed about 10 years ago by R.K. Chang at Yale together with researchers at the ARL [7, 8]. The aerosols are generated in a small reservoir equipped with an inlet (**I1**) injecting a 1 l/min clean air flow. The pollens in dry form are placed on the bottom of the reservoir together with a magnetic stirrer. The stirrer rotation speed regulates the particle concentration at the exit of the reservoir, which is connected to the experimental chamber. The latter is equipped with a specially designed sheath nozzle that has a second inlet of clean air (**I2**) with a flow of 1 l/min. The set up yields a focused laminar air flow of some 300 μm in diameter and 3 mm length. Single aerosol particles are simultaneously detected by two photomultipliers, monitoring the scattering from two crossed diode laser beams ($\lambda_1 = 780$ nm, $\lambda_2 = 655$ nm). The coincidence of both scattering signals generates a trigger pulse, sent to a constant frequency generator (**CFG**). This module creates the necessary TTL signals to synchronize the femtosecond laser to the particle flow. In our case, the Chirped Pulse Amplified (CPA) laser (Legend, Coherent Inc) provides pulses up to 2 mJ, 50 fs at 1 kHz repetition rate. It consists of a Kerr Lens mode locked oscillator (**LO**), a pulse stretcher (not shown on diagram), a regenerative amplifier cavity (**LC**) pumped by a 532 nm Q-switched Nd:YLF laser (**PL**), with an injection and an extraction Pockels cells (**PC1**, **PC2**), and a compressor (not shown on diagram). In our experiment, the clock for the Nd:YLF pump laser, is provided by the **CFG**. For each trigger event, the clock phase is readjusted in order to send a Nd:YLF pump pulse right after the trigger. The CPA is then synchronized by its own delay generator (**SDG**), which controls the injection of one femtosecond pulse into the regenerative amplifier and its extraction after amplification. A logic gate (**AND**) circuit prevents extraction of more than one pulse, so that each aerosol particle is illuminated by a single femtosecond pulse. The emitted MPEF is collected by a large aperture reflective objective (**L1**), dispersed by a grating (**G1**), and focused (**L2**) onto a 32-anodes PMT [8] (**D3**). The signal is finally acquired, stored, and analyzed by a spectrum acquisition electronic system (**SAS**).

3. Results and discussion

Figure 2 shows the MPEF images of the 3 selected pollens and the bacteria simulant acquired by a scanning microscope (Nikon A1R-MP) coupled to a Ti:Sapphire femtosecond laser oscillator (Newport Mai Tai HP DeepSee) tuned at 790 nm. MPEF is simultaneously detected by four independent non de-scanned photomultipliers set in four consecutive spectral channels defined by appropriate dichroic mirror/interference filter pairs. The actual spectral ranges correspond to UV (360 nm, FWHM 12 nm); Blue (485 nm, FWHM 20 nm); Green (531 nm, FWHM 40 nm), and Red (600 nm, FWHM 70 nm). When excited at 790 nm, pollens mainly absorb 2 photons and fluoresce in the blue-green channels, while FB345 clusters exhibit 3PEF in the UV

#154559 - $15.00 USD Received 13 Sep 2011; revised 11 Oct 2011; accepted 11 Oct 2011; published 15 Nov 2011

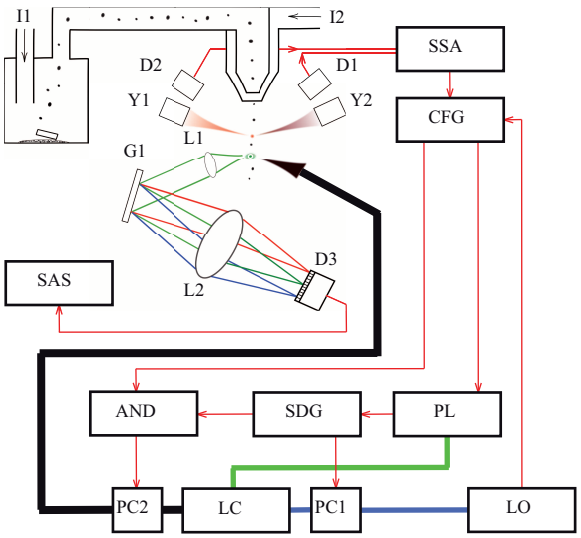

Fig. 1. Experimental set-up; **I1**, **I2** - air inlets; **Y1**, **Y2** - crossed diode lasers; **D1**, **D2** - spectrally filtered photomultipliers; **SSA** - scatter signal analyzer; **CFG** - constant frequency generator; **LO** - Ti:Sa femtosecond oscillator; **LC** - regenerative amplifier; **PL** - pump Nd:YLF laser; **PC1**, **PC2** - injection and extraction Pockels cells; **SDG** - system delay generator; **L1** - reflective objective; **G1** - grating; **D3** - 32-anodes PMT; **SAS** - spectrum acquisition electronics.

channel, as expected. At the typical incident intensity used 10^{12} W/cm^2, Ragweed exhibits a weak fluorescence in the UV channel too, in contrast to Pecan and Mulberry. This UV contribution clearly originates from 3PEF, in addition to the 2PEF in the blue-green channels. The laser intensity used in these experiments constitutes the upper limit before degradation of the samples. Notice that photomultiplier gain of each spectral channel was kept constant throughout the different samples to allow a visual comparison of the relative intensities. In particular, the UV channel gain was set to a very high value to detect the weakest signal intensities, as evidenced by the relatively large noise as compared to the UV case of series a). Pollen fluorescence is mainly attributed to NADH and to a smaller extent to flavins [19, 20]. Typical sizes of the pollens are respectively $19-20$ μm for Ragweed, $45-52$ μm for Pecan, and $12-13$ μm for Mulberry. The size of the airborne FB345 aggregates in the experiment was determined by elastic scattering from the crossed diode lasers to be 50 ± 30 μm.

The demonstration of the MPEF capability to discriminate between pollens and simulants of bacteria aggregates is shown in Fig. 3. Values on vertical axis represent number of photons seen by each pixel of 32-anode PMT. They are calculated from measured charges and 32-anode PMT typical sensitivity, and they are not corrected by optical response of filters, grating, optical windows and objective. For the chosen intensity of I $= 10^{13}-10^{14}$ W/cm^2, 2PEF of individual pollen particles and 3PEF of individual FB345 clusters are clearly detected and spectrally analyzed. Table 1 shows statistics of measured data. Due to the technical complications related to the synchronizing of a fixed repetition rate kHz CPA laser with the on-demand aerosol detection, less than 10% of scatter events rise to a spectral fluorescence detection. As compared to the MPEF microscopy experiment, higher intensities can be used since particle degradation is not a limitation (each particle is excited by a single femtosecond pulse). The spectra of the FB345 clusters (Fig. 3a) closely reproduce the reference curves of the doped polystyrene spheres with

#154559 - $15.00 USD Received 13 Sep 2011; revised 11 Oct 2011; accepted 11 Oct 2011; published 15 Nov 2011

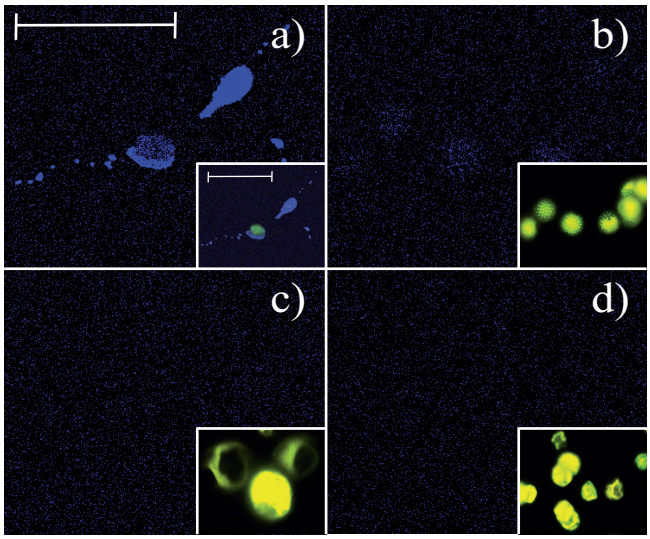

Fig. 2. MPEF microscopy images of a) FB345 clusters, b) Ragweed pollens, c) Pecan pollens, and d) Mulberry pollens. The large images correspond to the UV fluorescence channel (360 nm, FWHM 12 nm); the insets display the composite images of the UV- (360 nm, FWHM 12 nm), Blue- (485 nm, FWHM 20 nm), Green- (531 nm, FWHM 40 nm) and Red-channels (600 nm, FWHM 70 nm). The reference ruler corresponds to 50 μm.

a peak at 345 nm, well separated from the pollens 2PEF emission. The pollens spectra exhibit a broad maximum around 480 nm, in agreement with the characteristic emission of NADH, when excited by 2 photons at 790 nm [21]. However, significant differences are observed between the 3 pollen species. First, the emission maximum shifts from 440 nm (Ragweed, Fig. 3b) to 490 nm (Mulberry, Fig. 3d) with Pecan in between (470 nm, Fig. 3c). Secondly, the shapes of the spectra themselves differ. For instance Pecan and Ragweed exhibit significant fluorescence around 380 – 400 nm, which clearly originates from a 3PEF contribution. Mulberry emits only a weak fluorescence in this region (as also recorded in the microscopy images). These observations are in agreement with recent results obtained with the dual excitation fluorescence technique [9]. The authors indeed showed, that some pollens, especially Ragweed, exhibit fluorescence bands significantly shifted to the blue when excited at 263 nm as compared to the excitation at 351 nm. Conversely, Mulberry does not generate significant fluorescence around or below 400 nm, when excited in the UV. It appears thus that our spectra are a composite of the spectra observed with dual excitation schemes, i.e. a combination of 2PEF and 3PEF in pollens. Although not shown here, the ratio between the 2PEF and 3PEF components in the composite spectra could indeed be modified by tuning the incident laser intensity. As in the case of dual wavelength excitation, recording the whole spectrum instead of 2 fluorescence channels is of great help for discriminating between the particles. A significant improvement of our set-up in terms of sensitivity would be the excitation of the particles through the same objective as for the fluorescence collection, like in epi-microscopy. MPEF from individual aerosol particles is indeed strongly enhanced in the backward direction [22, 23] (up to a factor 10 for 3PEF). The important anti-Stokes shift between the 790 nm excitation and MPEF would allow efficient rejection at the dichroic beamsplitter.

In conclusion, we demonstrated for the first time that femtosecond laser pulses could generate detectable MPEF spectra from individual aerosol particles. This successful demonstra-

#154559 - $15.00 USD Received 13 Sep 2011; revised 11 Oct 2011; accepted 11 Oct 2011; published 15 Nov 2011

Table 1. Detection statistics

Sample	Scattering events	Emission peak, nm	Photon count for peak wavelength	Standard deviation
FB345	1248	350	543	75
Ragweed	712	445	503	35
Pecan	400	490	572	61
Mulberry	1285	490	1052	110

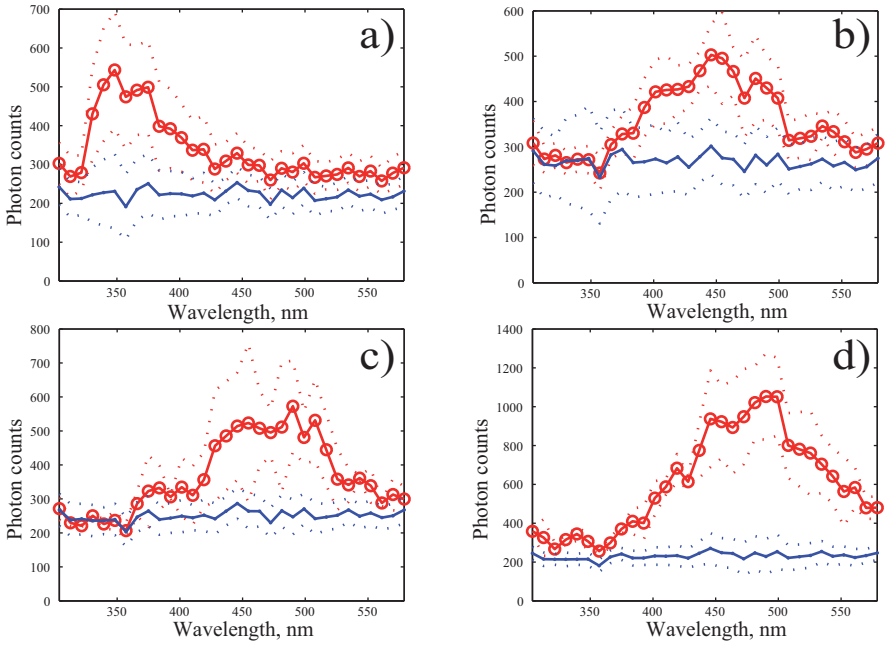

Fig. 3. Single-shot MPEF spectra of individual aerosol particles. (a) Simulants of bacteria aggregates (FB345); (b) Ragweed pollen; (c) Pecan Pollen; and (d) Mulberry pollen. The dashed lines represent the 96% confidence interval ($\pm 2\sigma$) calculated from a series of individual detection events.

tion experiment opens new possibilities for probing individual aerosol particles, namely femtosecond LIBS (Laser Induced Breakdown Spectroscopy) [24, 25], femtosecond pump-probe approaches that exploit differences in excited states dynamics [13, 14], coherent control of molecular wavepackets that proved able of discriminating molecules with identical linear spectra [16, 17], and femtosecond CARS (Coherent Anti-Stokes Raman Scattering) [26–29] that makes use of identified vibrational signatures.

Acknowledgments

We are grateful to Thibaud Magouroux for the Microscopy images on the Nikon multi-photon FP7 NAMDIATREAM platform. The authors wish to acknowledge the Swiss National Foundation for Research within the NCCR MUST program and the SER-COST action P21 (Physics of Droplets) for their support. They also wish to thank R.K. Chang (Yale), Y.L. Pan and S.C Hill. (ARL, Adelphi) for their advices in constructing the aerosol chamber, and for as well as E. Frejafon from INERIS for very fruitful discussions.

#154559 - $15.00 USD Received 13 Sep 2011; revised 11 Oct 2011; accepted 11 Oct 2011; published 15 Nov 2011